Supporting Information for

Compound effects of climate change on future transboundary water issues in the Middle East

Amin Dezfuli[1,2,*], Saman Razavi[3], and Benjamin F. Zaitchik[4]

[1] *Global Modeling and Assimilation Office, NASA Goddard Space Flight Center, Greenbelt, MD, USA*
[2] *Science Systems and Applications, Inc., Lanham, MD, USA*
[3] *School of Environment and Sustainability, University of Saskatchewan, Saskatoon, Canada*
[4] *Department of Earth and Planetary Sciences, Johns Hopkins University, Baltimore, MD, USA*

*Corresponding author (amin.dezfuli@nasa.gov)

Contents of this file

Text S1.

This document provides supplementary materials to support the results presented in the main body of the paper. Table S1 gives the list of 22 CMIP6 GCMs that have been evaluated. Based on the evaluation results presented in Fig. S1, 19 of these models have been selected for diagnostics analysis. Fig. S2 shows the difference between MME mean of these 19 GCMs and the observations to identify regions with highest and lowest agreement. Fig. S3 is used to find the delta values for bias correction of temperature and precipitation. Fig. S4 compares the histograms of temperature and precipitation of all three periods over the GAP region. It also shows the number of GCMs, contributing to each bin, so we can be reassured that the histograms are a fair representation of all models, and high frequency bins are not dominated by just one or two GCMs. Fig. S5 compares the annual cycle of temperature and precipitation over the GAP region for all three periods. To present the spread of the models, three percentiles (10th, median and 90th) of the 19 GCMs are also shown.
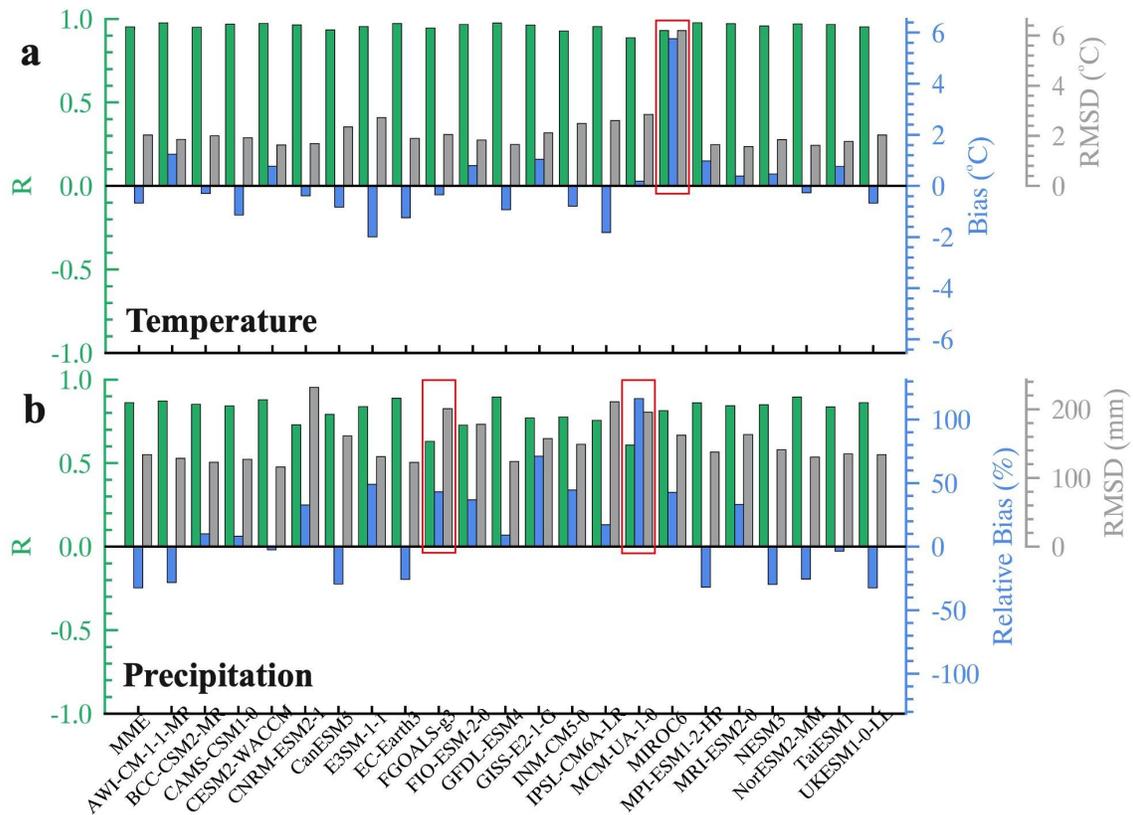
Figure S1. Evaluation statistics for **(a)** temperature and **(b)** precipitation over the baseline period (1981-2010), calculated for 22 CMIP6 GCMs and their multi-model ensemble (MME) mean. Temperature and precipitation used for evaluating the models are from MERRA-2 and GPCC, respectively. Pearson pattern correlation (R), root mean square difference (RMSD) and bias are calculated for land only grids. Note that for precipitation, "relative bias" is calculated as normalized percent difference.
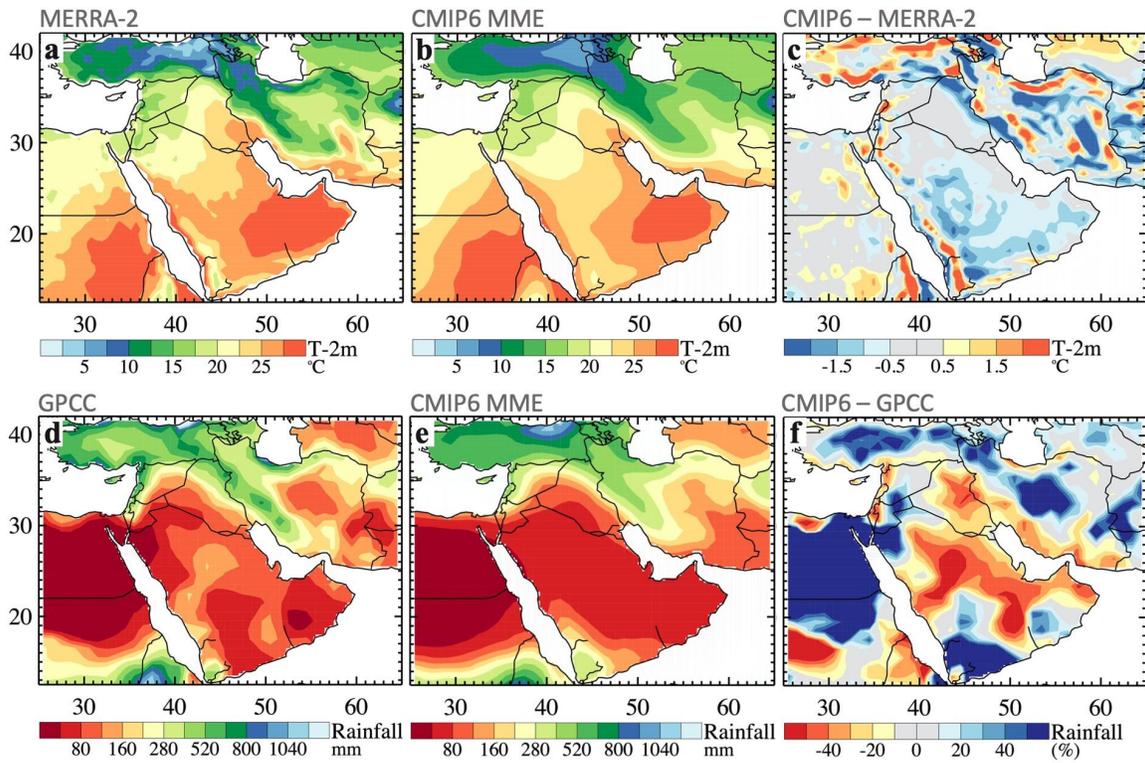
Figure S2. Long-term mean patterns of temperature (**a-c**) and precipitation (**d-f**). **a** and **b** are for MERRA-2 temperature and GPCC precipitation, respectively. The middle panels show the MME mean of 19 selected CMIP6 GCMs (see Data and Methods), and the difference between these and observations are shown in the right panels.
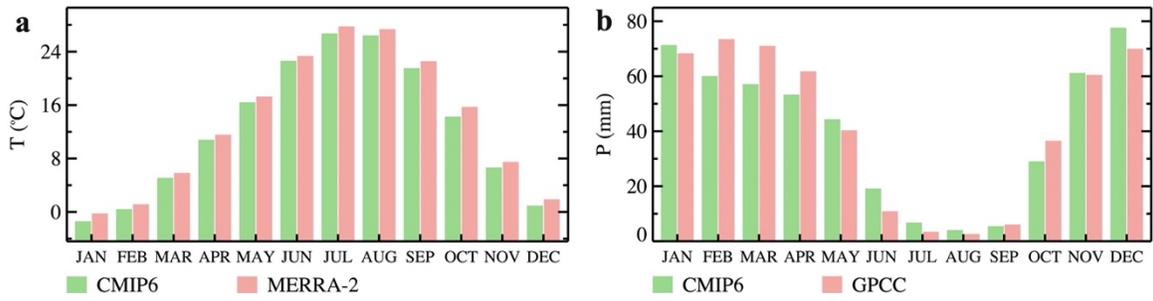
Figure S3. (**a**) Comparing the annual cycle of temperature from MERRA-2 and the MME mean of 19 selected GCMs for the baseline period (1981-2010), averaged over the GAP region. (**b**) The same as a but for comparing GPCC precipitation with the MME mean.
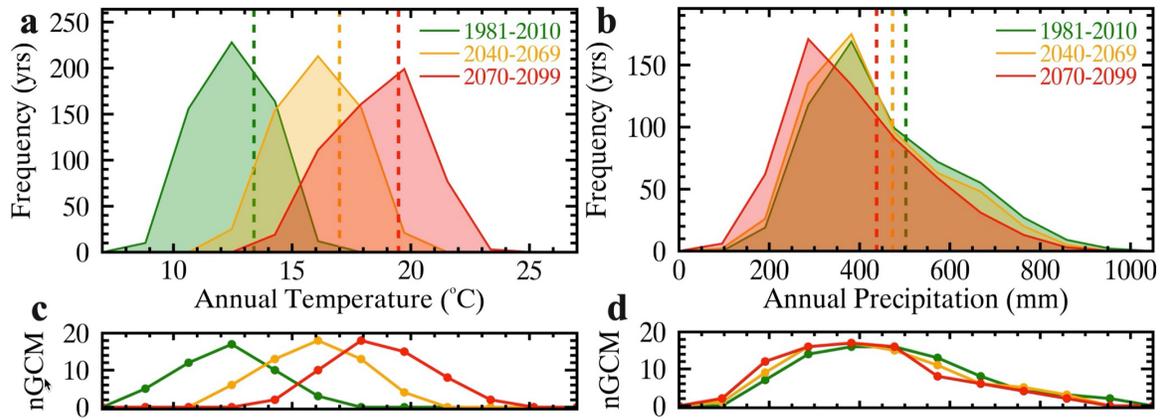
Figure S4. a and **b** are the same as Fig. 2, but also include the middle of the century (2040-2069). **c** and **d** show the number of GCMs that have contributed to each corresponding bin of the histograms for the three periods.
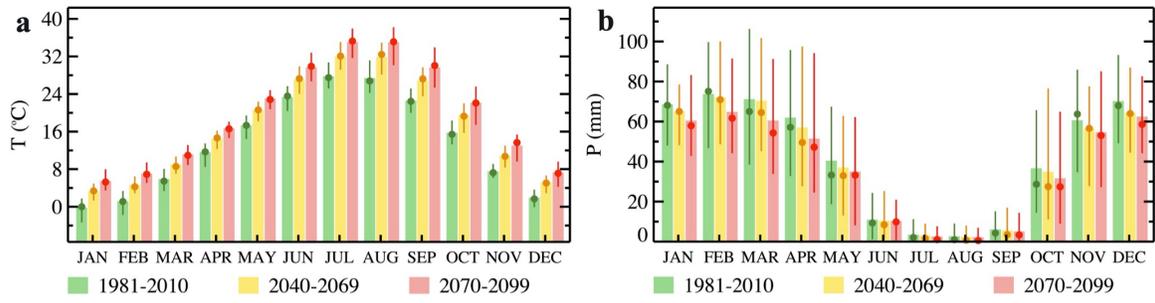
Figure S5. The same as Fig. 3, but also includes the middle of the century (2040-2069).

	GCM ID	Country	Horizontal resolution (lon x lat)	Selected
1	AWI-CM-1-1-MR	Germany	0.9˚ x 0.9˚	Yes
2	BCC-CSM2-MR	China	1.1˚ x 1.1˚	Yes
3	CAMS-CSM1-0	China	1.1˚ x 1.1˚	Yes
4	CanESM5	Canada	2.8˚ x 2.8˚	Yes
5	CESM2-WACCM	USA	1.25˚ x 0.9˚	Yes
6	CNRM-ESM2-1	France	1.4˚ x 1.4˚	Yes
7	E3SM-1-1	USA	1˚ x 1˚	Yes
8	EC-Earth3	Europe	0.7˚ x 0.7˚	Yes
9	FGOALS-g3	China	2˚ x 2.3˚	No
10	FIO-ESM-2-0	China	1.25˚ x 0.9˚	Yes
11	GFDL-ESM4	USA	1.25˚ x 1˚	Yes
12	GISS-E2-1-G	USA	2.5˚ x 2˚	Yes
13	INM-CM5-0	Russia	2˚ x 1.5˚	Yes
14	IPSL-CM6A-LR	France	2.5˚ x 1.25˚	Yes
15	MCM-UA-1-0	USA	3.75˚ x 2.2˚	No
16	MIROC6	Japan	1.4˚ x 1.4˚	No
17	MPI-ESM1-2-HR	Germany	0.9˚ x 0.9˚	Yes
18	MRI-ESM2-0	Japan	1.1˚ x 1.1˚	Yes
19	NESM3	China	1.9˚ x 1.9˚	Yes
20	NorESM2-MM	Norway	1.25˚ x 0.9˚	Yes
21	TaiESM1	Taiwan	1.25˚ x 0.9˚	Yes
22	UKESM1-0-LL	UK	1.9˚ x 1.25˚	Yes

Table S1. List of CMIP6 models evaluated.